

Generating coupled cluster code for modern distributed memory tensor software

Jan Brandejs ^{a)}, Johann Pototschnig , and Trond Saue 

Laboratoire de Chimie et Physique Quantique, UMR 5626 CNRS — Université Toulouse III-Paul Sabatier,
118 route de Narbonne, F-31062 Toulouse, France

(Dated: 25 February 2025)

Using GPU-based HPC platforms efficiently for coupled cluster computations is a challenge due to heterogeneous hardware structures. The constant need to adapt software to these structures and the required man-hours makes a systematization of high-performance code development desirable, even more so for higher-order coupled cluster. This is generally achieved by introducing a high-level representation of the problem, which is then translated to low-level instructions for the hardware using a compiler/translator component. Designing such software comes with another challenge: Allowing efficient implementation by capturing key symmetries of tensors, while retaining the abstraction from the hardware. We review ways to address these two challenges while presenting design decisions which led us to the development of a general-order coupled cluster code generator. The systematically produced code shows excellent weak scaling behavior running on up to 1200 GPUs using the distributed memory tensor library ExaTENSOR. We present an open-source modular tensor framework "tenpi" for coupled cluster code development with diagrammatic derivation, visualization module, symbolic algebra, intermediate optimization and support for multiple tensor backends. Tenpi brings higher-order CC functionality to the massively parallel ExaCorr module of the DIRAC code for relativistic molecular calculations.

I. INTRODUCTION

According to Jack Dongarra, the cofounder of the TOP500 list,¹ 99% of the FLOP performance of modern supercomputers lies in GPU accelerators.^{2,3} However, in the domain of distributed coupled cluster calculations, the focus of the present work, most implementations are able to use only about 10% of the theoretical maximum FLOP rate.⁴

This exposes the difficult situation in which scientists find themselves.^{5,6} Implementing fixed BLAS (Basic Linear Algebra Subroutines) and MPI (Message-Passing Interface) statements is no longer sufficient as modern machines have heterogeneous structures.⁷ Fig. 1 contains a schematic representation of a node of the Summit supercomputer. Communication throughputs and memory sizes differ between the components by orders of magnitude. Restructuring data movement across multiple levels of hierarchy to reduce the cost is a challenging problem,⁵ where the developer basically faces a graph theoretical task.⁸ The traditional 5-year lifespan of supercomputers⁹ has accelerated to about 3 years due to AI-driven breakthroughs in energy efficiency¹⁰ and keeping up with the changes requires expert manpower for which academia competes with industry.^{6,11}

The situation benefits systematic approaches to development and parallelization.^{5,13–15} One way is to build the code such that it can be quickly adapted to underlying numerical software changes using a code generator.^{13–15} Another way is to rely on tools which allow a high level of abstraction, like MATLAB,¹⁶ Maple¹⁷ or Mathematica,¹⁸ to write in parallel frameworks like SYCL¹⁹ and OpenACC,²⁰ to use runtime environments like StarPU,²¹ PaRSEC,²² MADNESS,²³ and LEGION,²⁴ or tensor compilers like DISTAL.²⁵

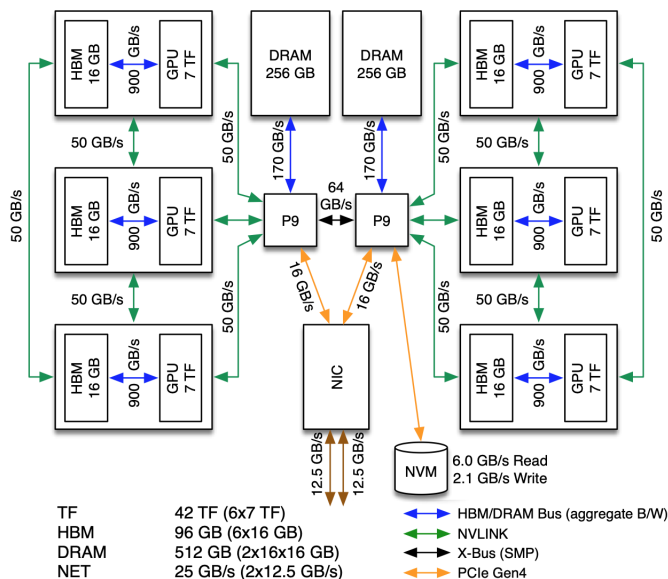


FIG. 1. Summit node structure. This figure is without copyright and is used after explicit consent by OLCF.¹²

In any case, one tries to i) abstract from hardware-specific code by using a high-level representation of the problem: creation/annihilation operator strings,¹³ their expansion using Wick's theorem,²⁶ diagrams,²⁷ tensor operations,²⁸ portable tasks²¹ and data distribution schemes.²⁵ ii) The software then translates this to instructions for hardware.

The challenge is to allow efficient implementation by capturing key mathematical features and symmetries of the problem, while retaining the abstraction from the hardware.²⁹ Strong candidates for finding this balance are tensor compilers²⁵ which have seen an explosion of interest³⁰ in the computer science (CS) community. However, to enable

^{a)}Electronic mail: jbrandejs@irsamc.ups-tlse.fr

production use in the coupled cluster domain, performance-critical features like index permutation symmetry or block sparsity would need to be implemented.^{27,31} The same holds for major machine learning libraries. Unlike in the case of AI, where big tech companies drive the development, in coupled cluster and tensor networks, scientists are left to rely on themselves. This was concluded at a panel discussion with representatives of these companies at a recent CECAM workshop³² which we co-organized.

The purpose of this paper is to explore the path from a high-level representation of CC methods to an efficient code on modern machines from the viewpoint of software-architecture. We provide the reader with a state-of-the art on the necessary tensor software, and we benchmark tenpi³³ - our solution to the two challenges: i) adapting CC to heterogeneous HPC, ii) identifying a balanced high-level representation.

A. Elegant development of CC methods, systematic approach

Equations in coupled cluster theory can reach a degree of complexity where manual manipulation is no longer practical.³⁴ Higher orders of the method with quadruple excitations and above include hundreds of terms with many indices. This accuracy is required to reach the scale of quantum-electrodynamics (QED) effects which our group is invested in.³⁵

Even though derivation by hand can be simplified by using diagrams which help detect equivalent terms, subsequent work with many indices is error-prone when done by hand. This and further manipulations like the design of intermediates with respect to a given cost-function³⁶ or implementing other flavors of the method are clear candidates for automatic symbolic treatment.

There have been numerous efforts in this direction with differing degrees of success. Here we focus on complete toolchains which include both equation and code generation - these are often linked to an existing quantum chemistry package. A prominent example and one of the pioneering systematization projects is the Tensor Contraction Engine (TCE)³⁷ initially developed by Hirata,¹⁵ a part of NWChem software.³⁸ Even though TCE was not the first such code generator,^{34,39-41} to the best of our knowledge, it has the most complete description in literature.¹³ Later works often follow its scheme.²⁷

1. Derivation (Derive the formulas of the method.)
2. Optimization (Optimize the expressions to reduce computational complexity.)
3. Transformation (Map to binary tensor contractions of a math library.)

Another noteworthy abstraction effort is the domain-specific language (DSL) SIAL (superinstruction assembly language) for tensor operations in the ACES III package.^{28,42} Even though initially successful, its limitation was the same as that

of TCE: customizability. Not all methods from the CC family can be efficiently expressed in the form of tensor contractions and without C++ or Fortran frontend support, one could not easily include custom code and optimizations.³¹ Some key parallelization optimizations even had to be done by hand in final Fortran loops of the generated code, as it was too difficult to modify the generator itself.⁴³ Further packages using their own tensor DSL include QChem⁴⁴ based on the libtensor⁴⁵ library, and Cyclops CTF⁴⁶ whose performance for distributed CPU contractions gained distinction in the computer science community, where it is used as a reference.^{25,47,48}

CC formula generators themselves divide in three main groups based on their approach to the derivation: i) by applying the algebra of creation and annihilation operators, ii) by Wick's theorem, iii) or by diagrams.

Unlike TCE, which was based on Wick's theorem, the derivation inside the MRCC package of Kállay and Surján³⁴ uses a representation of Kucharski-Bartlett diagrams^{49,50} based on strings of integers. In terms of derivation, the present paper builds on their approach.

The SMITH generator of Shiozaki^{27,51} is based on anti-symmetrized Goldstone diagrams.^{50,52} SMITH comes with an elegant input format in terms of second-quantized operators sandwiched between Slater determinants. Compared to its predecessors, SMITH is able to produce intermediates with index permutation symmetry for a broader class of methods.²⁷ The latest version 3 has transitioned from Wick's theorem to second-quantized operators and was used to generate parts of the BAGEL package.⁵³

Recent ORCA⁵⁴ is good example of a large-scale systematization effort where a substantial part of the package is generated using the ORCA-AGE generator¹³ based directly on application of the algebra of creation and annihilation operators. Even though this approach is very general, it took up to 7 years before performance issues with the generation were resolved.^{13,55}

New efforts have emerged in past years, as groups behind quantum chemical packages consider having their own toolchain. Most of them use Wick's theorem: i) SeQuant of the Valeev group²⁶ which is a C++ rewrite of their Mathematica code, ii) Drudge/Gristmill of the Scuseria group⁵⁶ which can switch between different abstract algebras and where the use of Wick's theorem is optional, iii) FEMTO of Saitow⁵⁷ used for DMRG-MRCI and pair-natural orbitals, iv) SQA⁵⁸, v) ebcc⁵⁹ and vi) GeCCo.⁶⁰ These efforts can be further classified by supported methods and features, see more detailed reviews.^{13,61} Many other efforts exist which focus on only one of the three steps of the process.^{40,62-65}

B. Optimization step

Algorithmically the most complicated part of the entire process is the automatic design of intermediates. Finding the optimal set of intermediates is NP-hard,^{13,66} so heuristics is used in practice. The ideal cost function would be the actual walltime of the target calculation, which depends on the size of the application system, the hardware and the underlying

math library. As this is unknown a priori, most optimizers rely on a naive FLOP count cost model, despite the fact that distributed CC calculations are often communication-bound, meaning that this model does not take into account the leading term of the walltime. Most chemistry codes are limited only to the basic single-term contraction path optimization and do not implement global (multi-term) optimization, which is replaced by hand-tuning.

The TCE also relies on search-based approach driven by a FLOP count performance model, using a global optimizer OpMin written by Sadayappan et al.³⁶ The optimization consists of:

1. Single term optimization (contraction path within a term)
2. Factorization (distributive law)
3. Common subexpression elimination (reuse equivalent terms)

This is a common structure among tensor contraction optimizers, with differing level of sophistication.³¹ OpMin performs well compared with hand-tuned code of NWChem for higher-order CC, also because its cost-function takes into account the index-permutation symmetry. Nevertheless, it does not support perturbative approaches with energy denominators.

Other efforts include a distributed GPU-contraction optimizer benchmarked for CCSD(T),⁵ followed by the AutoHOOT optimizer⁶⁷ (not CC), and an optimizer with a GPU-aware cost model.⁶⁸ The aforementioned complete toolchains also include own optimizers of varying levels of sophistication. For more information, see the literature overview in the thesis of Panyala³¹ on loop-level optimization.^{69,70} Note that there is no clear boundary on how low-level an optimizer should be. If it reaches low-level, it can be called a compiler, which is in fact a trend in state-of-the-art works.^{25,30,71} There is a strong connection between tensor compilers and compiler optimizations for different applications.⁷²⁻⁷⁴ However, CC contractions require specific treatment due to their distinctive features:³¹

1. A specific index permutation symmetry
2. Fully permutable *for* loops (order of summations)
3. Dependencies preventing loop fusion never occur

Last but not least, a noteworthy effort is the load balancer DLTC⁷⁵ which analyzes dependencies between contractions and groups them in layers that can be executed concurrently. This is particularly relevant for higher-order CC with large number of contractions with widely different computational cost.⁶¹

C. State-of-the-art: Tensor contraction

Tensor contraction represents the most computer-intensive operation of numerous methods in quantum chemistry, condensed matter physics, nuclear physics, machine learning and quantum computing.⁷⁶⁻⁷⁸ Examples include coupled cluster methods,^{4,22,79} tensor networks,⁸⁰ quantum computing

simulators,⁸¹ certain neural networks⁸² and signal processing methods.^{83,84} Common to all these is that the key limitation to the affordable system size is the cost of tensor contraction.

Typically, the software packages decompose tensor contractions into primitive matrix operations and pass them to BLAS.^{85,86} There are different approaches of dealing with tensor transposition (reshape), which is in general required for the usage of BLAS GEMM (General Matrix Multiplication), which depends on a unit-stride index to multiply two matrices. Given a tensor memory layout, an index is said to have a unit stride when incrementing it by one translates to a move by one scalar in memory. Note that in the context of tensor operations, the CS community uses the term transposition interchangeably with reshape. The most common approach is TTGT⁷⁷ (Transpose-Transpose-GEMM-Transpose): for $C = A \times B$

1. Transpose A and B into unit-stride form
2. Use GEMM to execute the contraction
3. Transpose result array to obtain C

In his block-scatter matrix tensor contraction (BSMTC) scheme, Matthews⁷⁷ has shown that is possible to hide the transposition cost by loading tensor parts into CPU L2 and L3 cache in order which effectively performs the required permutation of its elements.

Another alternative is the GETT scheme (GEMM-like tensor-tensor multiplication) by Springer and Bientinesi⁸⁷ which generates code to call matrix-matrix multiplication kernels while again reformulating the sub-matrix-packing. A GPU implementation thereof has become a foundation of the single-node library cuTENSOR.⁸⁸

Regarding the parallelization strategy, most software relies on OpenMP+MPI parallelization on homogenous CPU-based computational clusters.⁴ The advent of GPU-based supercomputers has rendered this paradigm obsolete.²²

Comparing to the software for matrix operations, we currently identify two major practical hurdles for tensor software:

1. Contrary to BLAS for matrix operations, there is no standardized interface for tensor operations. This causes substantial code duplication.⁷⁶
2. Contrary to CPU-based software,^{46,79} there is no established GPU-based implementation of a tensor contraction library with support for features required by the community such as distributed memory and block sparsity,²² which would offer sufficient level of maintenance and optimization for current supercomputers.

As for standardization, there has been some work in the past, but none of the interfaces have prevailed. BTAS⁸⁵ has aimed at providing a standard and a basic CPU implementation. TBLIS⁷⁷ provides BLAS-like tensor calls. Until today, there is no GPU implementation of these. During the 2022 Dagstuhl tensor workshop,⁸⁹ a development of domain-specific tensor language has been initiated, but remains unfinished and undocumented. There has been work-technical specifications of additional aspects of standardization, like tensor-memory distribution^{90,91} and randomized multilinear algebra.⁹² Currently, there are recurring meetings

across academia and private sector under the TAPP (Tensor Algebra Processing Primitives) standardization initiative.⁹³

Regarding the implementations, there are numerous scattered efforts listed in Ref. 76. However, for open-source distributed memory GPU libraries, there are only a few major players. i) ExaTensor^{7,94} based on TAL-SH⁹⁵, where the key developer has left to industry. ii) TiledArray⁷⁹ and Cyclops CTF,⁴⁶ where the solid support for GPUs is still under development. iii) TACO DISTAL,²⁵ which has performance issues for higher-order tensors. iv) TAMM⁹⁶ scales well on supercomputers, but has a potentially problematic dependency of Global Arrays,⁹⁷ with a small user base for a communication library. v) cuTensor^{88,98} is proprietary and only supports Nvidia hardware, while vi) hipTensor⁹⁹ is at an early stage of development. Other industry products like vii) PyTorch¹⁰⁰ and viii) TensorFlow¹⁰¹ focus almost exclusively on machine learning and again lack features required in CC.

II. THEORY AND IMPLEMENTATION

A. Coupled cluster amplitude equations and their generation

The coupled cluster method is based on an exponential ansatz

$$|CC\rangle = \exp(\hat{T})|\Phi_0\rangle, \quad \hat{T} = \sum_{\ell} t_{\ell} \hat{\tau}_{\ell} \quad (1)$$

where $\hat{\tau}_{\ell}$ is an excitation operator, and t_{ℓ} the corresponding cluster amplitude tensor. Φ_0 in our case denotes the Hartree–Fock (HF) reference.

Even though the code generator is designed to go to arbitrary order and in practice generates optimized code up to CCSDTQP (see Table I), in the presented applications we restrict ourselves to up to quadruple excitations

$$\begin{aligned} \hat{T} &= \hat{T}_1 + \hat{T}_2 + \hat{T}_3 + \hat{T}_4, & \hat{T}_1 &= \sum_{ai} t_i^a a_a^\dagger a_i, \\ \hat{T}_2 &= \frac{1}{4} \sum_{abij} t_{ij}^{ab} a_a^\dagger a_b^\dagger a_j a_i, & \hat{T}_3 &= \frac{1}{36} \sum_{abcijk} t_{ijk}^{abc} a_a^\dagger a_b^\dagger a_c^\dagger a_k a_j a_i, \\ \hat{T}_4 &= \frac{1}{24^2} \sum_{abcdijkl} t_{ijkl}^{abcd} a_a^\dagger a_b^\dagger a_c^\dagger a_d^\dagger a_l a_k a_j a_i. \end{aligned} \quad (2)$$

We use i, j, k, l and a, b, c, d to denote occupied and virtual orbitals respectively.

After defining the similarity transformed normal-ordered Hamiltonian as $\bar{H} = \exp(-\hat{T})\hat{H}_N \exp(\hat{T})$, we can write down the CC energy equations

$$\begin{aligned} \langle \Phi_0 | \bar{H} | \Phi_0 \rangle &= E - E_{HF}, \\ \langle \Phi_{\ell} | \bar{H} | \Phi_0 \rangle &= 0, \quad \text{with } |\Phi_{\ell}\rangle = \hat{\tau}_{\ell} |\Phi_0\rangle, \end{aligned} \quad (3)$$

which determine the energy and the cluster amplitudes.

The explicit equation terms can then be derived using different techniques. In our implementation, we chose the diagrammatic scheme of Kállay and Surján³⁴ (see the reasoning in Section II B). This general-order coupled cluster derivation

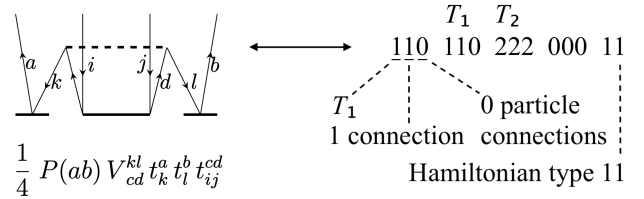


FIG. 2. The string representation of CC diagrams, an example. The three consecutive zeros are to leave space for one further admissible \hat{T} operator. Note that the triplets of integers corresponding to \hat{T} operators are ordered to assure uniqueness of the diagrams. See Ref. 34 for a full explanation. Left: Visual representation of a diagram and an equation shown as printed from tenpi.

Using convention $(\mu_1, \mu_2, \mu_3) = (T \text{ operator level, number of connections, number of particle connections})$

- 1: $k \leftarrow$ excitation level of the projection determinant
- 2: $n \leftarrow$ maximum excitation level of individual T -operators
- 3: **for each** $l \leq 4$, with l the number of T operators **do**
- 4: μ_1 : All positive l -tuples with sum between $k-2$, $\min(k+2, n)$
- 5: Comment: One l -tuple contains l numbers of type μ_1 to
- 6: appear in a single diagram
- 7: **for each** candidate l -tuple of μ_1 's **do**
- 8: **for each** Hamiltonian type matching excitation level **do**
- 9: μ_2 : All l -partitions of the number of internal
- 10: lines between 1 and $2\mu_1$ (the corresponding μ_1)
- 11: **for each** candidate l -tuple of μ_2 's **do**
- 12: μ_3 : All l -partitions of the number of particle
- 13: internal lines between 0 and $\min(\mu_1, \mu_2)$
- 14: **for each** candidate l -tuple of μ_3 's **do**
- 15: Keep the candidate diagram string if its l
- 16: integer triples are mutually sorted ascen-
- 17: dingly (their corresponding components).
- 18: **end for**
- 19: **end for**
- 20: **end for**
- 21: **end for**
- 22: **end for**

FIG. 3. A simple algorithm to generate diagram strings as shown in Fig. 2 for the CC Eqs. (3). Please refer to the original Ref. 34 for a detailed description. This algorithm has been extended in tenpi to support matrix elements with any bra and ket excitation levels, arbitrary interaction, excitation and de-excitation operators or $\exp(\hat{T})$.

scheme is based on a **string representation of CC diagrams**. As depicted in Fig. 2, an integer string of length 13 is used to represent a diagram. Two diagrams are equivalent up to a sign if their strings are the same. There is a simple algorithm depicted in Fig. 3 that uses this representation to generate distinct diagrams for each excitation level of the CC Eqs. (3).

To find the explicit equation terms, tenpi³³ translates the integer strings into line graph representation, i.e. an edge list of particle and hole lines connecting operators and external bra indices of Eqs. (3). Such a representation makes the application of coupled cluster interpretation rules similar to when done by hand. All used high-level representations are summarized in Fig. 5 and explained in Sections II B and II C.

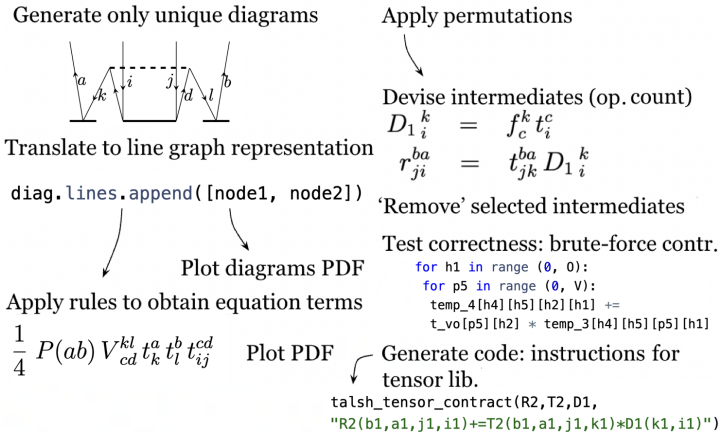


FIG. 4. The workflow of tenpi. First, diagrams are generated. These are then translated to a line chart representation. The CC interpretation rules are applied and both diagrams and equation terms are printed in a textbook-like PDF format. The permutations are applied and resulting code is optimized using OpMin. The produced intermediates are reoptimized to decrease memory cost using the algorithm in Fig. 6. The correctness of intermediates is tested using generated simplistic brute-force python script. Equations are printed in readable format in each of these steps. The entire source code files are generated as required (ExaTENSOR FORTRAN, NumPy python, etc.). The procedure can be fully customized as all these steps are calls to the high-level interface of the tenpi python library.³³

B. Design decisions

The initial goal of the tenpi project was to create a programming environment for relativistic coupled cluster which separates science from the computational platform by getting tensor developments under the hood. This has three aspects:

1. Systematic development of higher-order coupled cluster methods which include hundreds of tensor contractions.
2. Development without having to consider the parallelization strategy.
3. Automatic treatment of tensor symmetries, such as index-permutation symmetry and block-sparsity (for systems with spatial symmetry).

This paper addresses the first two points and prepares the ground for the third point.

The design choices are limited by practical considerations. The toolchain should not be restricted to a given flavor of the coupled cluster method, but should be written in a general way and be able to go to high orders of the theory. It should allow manipulations of the method by PhD and Master students of quantum chemistry. This led to the decision to base the formula generator on **Kucharski-Bartlett diagrams**,^{49,50} since diagrams are visual and thus more accessible for students than the other CC derivation schemes listed in section I A. The ease of use for target users is one of the reasons why we chose **python** to implement the generator, aside from the fact that it is suitable for text processing and symbolic operations. The **string representation of CC diagrams** of Kállay and Surján³⁴ was chosen because it clearly distinguishes

equivalent diagrams and can be used to generate distinct connected diagrams (see section II A) in an intuitive way.³⁴

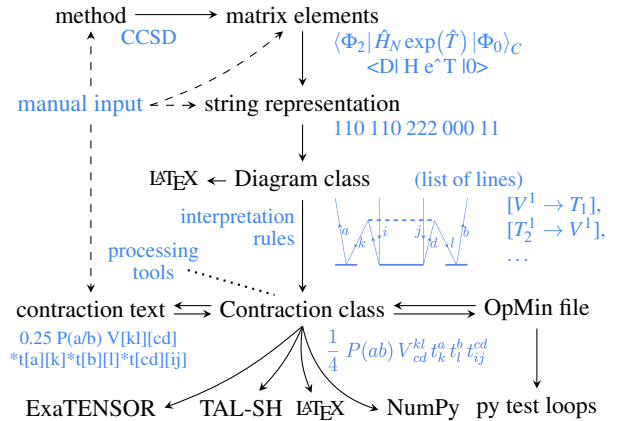


FIG. 5. High-level representations of the problem in the tenpi implementation. An example is found on the bottom-right of most representations in blue. Solid arrows between representations show implemented conversions, which typically follow the workflow of the program. Dashed arrows indicate the four possible entry-points for user input. Once one uses tenpi as a library or in interactive regime, a broad class of customizations becomes available, e.g. adding energy denominators to selected terms or contracting open lines of two diagrams together to get a scalar. Output code is in the bottom row. The second blue line under matrix elements shows how is the example matrix element actually input. Superscript in the list of lines under Diagram class numbers the nodes of an operator. The list of lines represents a directed graph corresponding to the diagram. Contraction class is a central representation in the code. It features a range of processing tools for symbolic manipulations on a set of equations, like substitution of terms, their products, contraction of terms, index permutations and detection when a tensor can be deallocated. Brute-force python test loops serve to check numerically the equivalence of two sets of equations (see section II C).

The diagram strings are next translated into **directed graphs**, by storing a list of edges (adjacency matrix). This representation makes the implementation of the CC interpretation rules readable. Advanced users can define a custom set of rules (customizability) or for instance extend the Diagram class to support multiple interaction operators and other generalizations, without having to change the rest of the code (modularity).

To follow closely the hand-typeset style of the pedagogical texts of Refs. 102 and 49, tenpi prints the diagrams in PDF format using the CCDiag LaTeX package.¹⁰³ During the development of higher-order CC methods this **visual representation** proved itself invaluable for debugging. Overall, the emphasis on intuitive, readable, modular and visual implementation makes problems directly visible and modules unit-testable (see section II C).

The workflow of the tenpi code generator is depicted in Fig. 4 and corresponding high-level representations in Fig. 5. A key step is to **optimize the expressions** obtained. Since writing a global optimizer from scratch is beyond the scope of this work, we interfaced our code with OpMin, which was chosen over Gristmill⁵⁶ due to a favorable performance

for higher-order CC.³⁶ However, even though the heuristics of OpMin is reported to stay within 3% of the global minimum FLOP-count, the number of intermediates it generates tends to be too costly in terms of memory. Higher-order CC tensors in our calculations cannot be stored on disk due to prohibitive I/O costs. Our approach is to distribute them among the CPU and GPU RAM memory of the nodes. This comes with a limitation in the amount of available distributed memory due to communication overhead growing quadratically with the number of nodes in the round-robin distribution scheme used (see below). Therefore, we implemented our **own secondary optimization**, which rolls back part of the intermediates by plugging them back in their respective terms. The number of intermediates is reduced by about a factor of three at the expense of increasing the FLOP count (see Fig. 6). This approach is justified as long as the calculation stays communication-dominated. We do not reach a perfect balance, which would require setting up a communication-based cost-function. Optimization of this aspect is the subject of ongoing work.

During the optimization, we originally represented contractions using the SymPy package¹⁰⁴ but later we turned to the use of a **custom representation of tensor contractions** for greater flexibility (Contraction class, see section II C). Even though SymPy is widely used, its current user interface is cumbersome for higher-order tensors.

The accessibility of the code should not come at the cost of performance. Therefore, the generated production code is strictly in a compiled language, in our case **Fortran 2008** in order to integrate smoothly with the ExaCorr module⁹⁴ of the DIRAC package.^{105,106}

As we aim for scalability on modern GPU exascale machines, we turned to the use of a **tensor library** to execute the final tensor kernels (ExaTENSOR, TAL-SH). ExaTENSOR was chosen from the limited list of available distributed GPU tensor libraries (see section II C) due to its excellent performance for relativistic CCSD.⁹⁴ In the present work, the performance is reproduced and demonstrated to scale to up to 1200 GPUs by automatically generated code (see Fig. 9).

C. Implementation

An equation term is implemented using the ‘Contraction’ class, which includes a list of tensors, a scalar factor and optionally permutation operators and an output tensor. Contraction class instances are collected in a list, which forms the left-hand side of Eqs. (3).

Tensor class includes a list of upper and lower indices. Each index is an Index class instance. Index class has its type (e.g. occupied, virtual, active virtual), a convention according to which it is printed (e.g. $a, b, i, j; p_1, p_2, h_1, h_2$) and then a number corresponding to the order in which the specific character comes in the class (e.g. $a \mapsto 1, b \mapsto 2, h_1 \mapsto 1$). Types and conventions are easily customizable by modifying a single location in the code, which greatly facilitates the implementation of methods and symmetries with multiple index spaces or tiling.⁹⁶ Index, Tensor and Contraction class are fully com-

```

1: repeat
2:   if intermediate defined in a single operation then
3:     if it is always used in additions then
4:       plug it back in
5:     end if
6:   end if
7:   if intermediate used only once then
8:     if its definition only contains additions then
9:       plug it back in
10:    else if it is used in an addition then
11:      plug it back in
12:    end if
13:  end if
14: until no change since the last iteration

```

FIG. 6. Secondary optimization of intermediates to help restore the balance between the memory cost and operation count by removing eligible intermediates (plugging them back in the equation). Each time indices have to be permuted accordingly. The scheme is limited by the need to avoid contractions of more than two tensors to keep the instructions compatible with ExaTENSOR.

patible with smart functionality to account for block-sparsity in tensors and to keep track of index permutation symmetry in intermediates explicitly. Work is in progress to include this functionality in the production code. A set of equations can **switch between conventions** with a single command. This is important because tenpi supports multiple input and output formats to interface with ExaTENSOR, TAL-SH, OpMin, NumPy, including a possibility to input equations by hand (see Fig. 5). For the sake of modularity, all these codes are integrated by extending one of two predefined interfaces: GetCodeInterface or ParseCodeInterface. These specify how to implement a new format of output or input respectively. Thanks to this design it is **straightforward to interface** tenpi with a new program.

The optimization of intermediates is an error-prone procedure and checking the results by hand can be extremely tedious. Therefore, following the example of OpMin, tenpi includes verification of correctness using a generated python brute-force test code with contractions expressed in nested *for* loops. Random tensors with tiny virtual and occupied sizes are used to check whether the optimized equation produces the same result as the original one.

The derivation step of tenpi is very fast, see timings in Tab. I. We have verified by comparing with Ref. 34 that tenpi generates the correct number of diagrams for each of the CC Eqs. (3) up to excitation level 20. Even though it generates a highly-parallel code, tenpi itself is written as sequential python. Despite this, the most demanding step of global intermediate optimization still performs quite well.

Aside from amplitude equations, tenpi can already generate matrix elements (see Figs. 3, 5, cf. SMITH^{27,51}) and is currently being extended to generate response density matrices.

When going from CCD and CCSD levels during the development, an error in energy appeared. It was found quickly thanks to the visual representation of diagrams: For the CC

method	CCD	CCSD	CCSDT	CCSDTQ	CCSDTQP
number of diagrams	11	48	102	183	289
derivation step	0.03 s	0.1 s	0.3 s	0.6 s	0.8 s
OpMin	0.03 s	40 s	22 min	7 h 10 min	4 days 1 h
2nd optimization	0.02 s	0.1 s	16 s	1 h 9 min	17 days
code generation	0.01 s	0.1 s	3 s	2 min	2 h 13 min

TABLE I. Timings of generation of high-performance code by tenpi, which is itself a sequential python implementation. If needed, the secondary optimization step can be made several times faster relatively easily by having the algorithm modify multiple terms in one pass. We chose to have it modify just a single term per pass as this was less error-prone during the initial development phase. In contrast to that, improving the performance of OpMin would be quite hard.

diagram interpretation rules to yield a correct sign, e.g. for the case of amplitude-equation projected onto $|\Phi_{ij}^{ab}\rangle$, the line starting in i has to end in a , and not in b . This rule is often assumed implicitly.^{49,102} Transition from CCSDT and CCSDTQ proved to be more peculiar, due to a mistake in an algorithm for unrolling index permutations. The problem was unraveled once a brute force unit test was written for the corresponding module.

III. COMPUTATIONAL DETAILS

A. Machines used

The calculations were performed on the machines listed in Table II which includes their technical specification. When ExaTENSOR is applied for coupled cluster,⁹⁴ the most relevant parameters for the performance are the interconnect bandwidth, RAM (random-access) and HBM (high-bandwidth) memory, as well as GPU specifications. Over the two supercomputer generations represented in Table II the bandwidth and the HBM have grown about fourfold, while RAM has basically stagnated. Despite the rapid development of GPU processing power, the table shows that the evolution of other important parameters has been relatively slow over the last 5 years. Recently, large memory CPU nodes have emerged which go against this trend, e.g. Intel Xeon 6900P with MRDIMM technology (Multiplexed Rank Dual In-line Memory Module) and 3 TB of fast memory as announced for an HPC platform in Japan.¹⁰⁷

We would like to bring to the attention of the reader that one should not expect an easy installation and tuning of distributed memory tensor libraries, as it mostly requires GPU and MPI experts. ExaTENSOR features cutting-edge parallelization strategy with multithreading, nested OpenMP threads, GPU-aware MPI and one-sided communication, which proved itself difficult to support for some HPC platforms. For instance on Frontier, an internal resource starvation within Cray MPICH¹⁰⁸ causes certain MPI requests to be blocked, and the calculation hangs as a result. The engineers from the supplier company (HPE) are currently working on the issue.

B. Relativistic Hamiltonian

The state-of-the-art post-HF four-component relativistic calculations employ the no-pair approximation.^{109,110} This approximation is well-substantiated for applications of chemical scale. Formally, it yields a Hamiltonian analogous to the non-relativistic case

$$H = \sum_{pq} h_p^q a_p^\dagger a_q + \frac{1}{4} \sum_{pqrs} \langle pq || rs \rangle a_p^\dagger a_q^\dagger a_s a_r, \quad (4)$$

where the indices p, q, r, s only run over the positive-energy spinors that span the one-electron basis.

In the present work we employ, unless otherwise stated, the exact two-component (X2C) Hamiltonian,^{111–114} where the summations in Eq. (4) are limited to positive energy orbitals by construction. Relativistic two-electron picture-change corrections were added either using the AMFI package^{115,116} or using the recently implemented amfX2C (XAMFI) correction.¹¹⁷ The Gaunt/Breit terms are not included in the present work.

C. Geometry, basis, etc.

For the benchmarks, we used the UF₆ molecule in dyall.v2z basis¹¹⁸ with the X2C Hamiltonian, and bond distance of 2.077521 Å. In the corresponding ground-state energy CC calculations, we used a HF reference. Despite the high O_h symmetry, there is no related performance gain in the CC calculations as the implementation does not support symmetry yet.

Furthermore, we studied CO in cc-pVTZ basis¹¹⁹ at bond-distances between 0.8 and 1.85 Å. There, we used the amfX2C correction for two-electron scalar-relativistic and spin-orbit picture-change effects arising within the X2C Hamiltonian framework.¹¹⁷

For the cases where the full virtual space is not used, we then calculated the MP2 frozen natural orbitals¹²⁰ (with a cutoff on occupation number) on top of which the final CC calculation was done.

We performed two correctness checks with a nonrelativistic Hamiltonian. For the first test, we chose H₂O in a 3-21G basis¹²¹ at the equilibrium internuclear distance of 0.975512 Å and H-O-H angle of 110.565°. The second test is with LiH in 6-31G basis^{122,123} at the internuclear distance of 1.6 Å. Both CC correctness tests were performed with respect to the HF reference.

All the CC calculations were performed in uncontracted basis sets. When referring to sizes of occupied and virtual spaces, we use the notation of AS(k, n), where k is the number of electrons and n is the number of Kramers pairs active in a coupled cluster calculation (occupied+virtual). One Kramers pair corresponds to two spinors related by time reversal symmetry. In all calculations, the choice of occupied and virtual spaces respects the rising orbital energies or the occupation numbers in the case of MP2. See the used software in Section IV A.

machine	Frontier	LUMI	Karolina	Summit	Olympe
laboratory organization	OLCF U.S. DOE	CSC data center EuroHPC	IT4Innovations Cz. edu. ministry	OLCF U.S. DOE	CALMIP CNRS
GPU nodes	9408	2978	72	4600	48
GPUs per node	8	8	8	6	4
GPU type	AMD MI250x	AMD MI250x	NVIDIA A100	NVIDIA V100	NVIDIA V100
HBM per GPU	64 GB	64 GB	40 GB	16 GB	16 GB
CPU type	AMD EPYC 7713	AMD EPYC 7A53	AMD EPYC 7452	IBM POWER9	Intel Skylake
cores per node	64	64	64	168	36
RAM per node	512 GB	512 GB	1024 GB	512 GB	384 GB
network	Cray Slingshot	Cray Slingshot-11	Infiniband HDR200	Infiniband EDR	Infiniband EDR
net. bandwidth	4x 25 GB/s	4x 25 GB/s	4x 6.25 GB/s	23 GB/s	12.5 GB/s

TABLE II. GPU-based HPC platforms used for the calculations and their corresponding technical specifications.¹

IV. RESULTS AND DISCUSSION

A. Correctness: H₂O and LiH

To demonstrate the correctness, we compare ground state coupled cluster energies from tenpi (present work) with the established MRCC package^{34,124–126} and with existing handwritten code in DIRAC^{105,106} where possible, i.e. either with the initial DIRAC RelCC module¹²⁷ or with the more recent massively parallel ExaCorr module.⁹⁴ The correctness check was performed on two small systems: H₂O (Table III) and LiH (Table IV) and shows an agreement within the convergence error.

method	code	convergence ^e	Total energy [E_h]
SCF	DIRAC SCF	1.1E-12 ^a	-75.58 5498 7542
SCF	MRCC	4.4E-13 ^a	-75.58 5498 7680
MP2	DIRAC ExaCorr		-75.66 6586 2130
MP2	MRCC		-75.66 6586 2218
CCSD	DIRAC tenpi ^d	0.5E-09 ^c	-75.67 2947 6512
CCSD	MRCC	9.6E-10 ^c	-75.67 2947 6563
CCSDT	DIRAC tenpi ^b	0.4E-09 ^c	-75.67 3875 1038
CCSDT	MRCC	4.9E-10 ^c	-75.67 3875 1087
CCSDTQ	DIRAC tenpi ^b	0.1E-08 ^c	-75.67 3974 4768
CCSDTQ	MRCC	3.5E-10 ^c	-75.67 3974 4817

TABLE III. Correctness check on the ground state energies of H₂O. AS(6, 11). Calculated on Olympe.

- ^a energy difference
- ^b using the ExaTENSOR library
- ^c norm of the residual vector
- ^d using the TAL-SH library
- ^e the final error shown in the run

B. Benchmark: UF₆ CCSD

To benchmark the parallel scaling, we compare the performance of CCSD generated by tenpi with hand-tuned code in the ExaCorr module of DIRAC and with generated code from the *codegen* (mb-autogen) generator.¹²⁸ First we perform a strong-scaling benchmark on UF₆ with fixed problem size. In

method	code	convergence ^d	Total energy [E_h]
SCF	DIRAC SCF	1.4E-12 ^a	-7.97 9321 5650
SCF	MRCC	6.2E-15 ^a	-7.97 9321 5634
MP2	DIRAC ExaCorr		-7.99 1935 0613
MP2	MRCC		-7.99 1935 0593
CCSD	DIRAC tenpi ^b	0.6E-09 ^c	-7.99 8346 9438
CCSD	MRCC	2.9E-10 ^c	-7.99 8346 9410
CCSDT	DIRAC tenpi ^b	0.5E-09 ^c	-7.99 8358 3476
CCSDT	MRCC	4.2E-10 ^c	-7.99 8358 3449
CCSDTQ	DIRAC tenpi ^b	0.3E-05 ^c	-7.99 8358 3478
CCSDTQ	MRCC	7.0E-10 ^c	-7.99 8358 3630

TABLE IV. Correctness check on LiH. AS(4, 11). Calculated on Olympe.

- ^a energy difference
- ^b using the ExaTENSOR library
- ^c norm of the residual vector
- ^d the final error shown in the run

all cases, the correct total energy of $-28638.655880 E_h$ is retrieved with residual norm less than 0.8×10^{-6} . The parallel speedup for strong scaling benchmark is calculated in a standard way as a walltime ratio t_1/t_N for N processing units (in this case we consider entire nodes). If t_1 is not available due to large memory requirements, the timing per node with the minimal number of nodes is used to estimate it.

The benchmark was performed on the Summit supercomputer of the Oak Ridge Leadership Computing Facility (OLCF) using the GPU implementation of the ExaTENSOR library. Each Summit node is equipped with 6 GPUs (see Table II). We used up to 300 GPUs simultaneously for strong scaling.

As shown in Fig. 7, the code scales well until about 20 nodes for UF₆. There, the curve leaves its approximately linear behavior. This is expected for fixed problem size. As the number of workers increase, they start to suffer from work starvation, which eventually causes the overhead from the unnecessarily increased internode communication to dominate. We chose to model this using the Amdahl's law¹²⁹ for strong scaling

$$\text{speedup} = \frac{1}{s + p/N}, \quad (5)$$

where N is the number of nodes, s and p are the proportions of serial and parallel code. From fitting, we found $s = 5.5\%$, corresponding to when the processes wait for communication during tensor operations and for synchronization barriers which are enforced after each tensor operation.

As expected, the automatically generated code is slightly less efficient than the hand-tuned code. The timings in Fig. 8 show a fixed-factor slowdown of about 30% for tenpi, whereas about 80% for *codegen*. The former is a good result when compared with ORCA, where 100% timing overhead was a practical rule of thumb threshold for acceptance of generated code.¹³

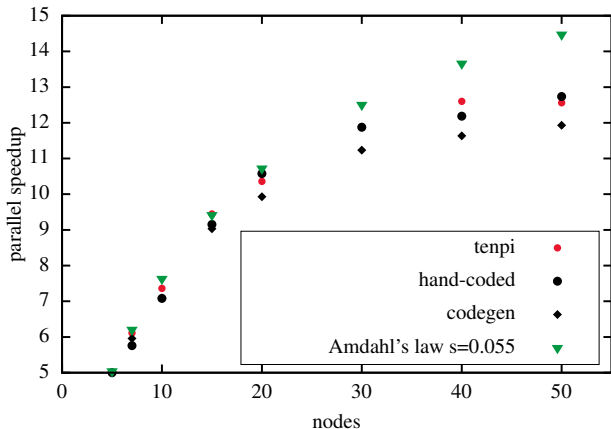


FIG. 7. Strong scaling benchmark on UF_6 . Average parallel speedup for a relativistic CCSD iteration (relative to the smallest possible run) with respect to the number of Summit nodes (6 GPUs per node). AS(66, 190).

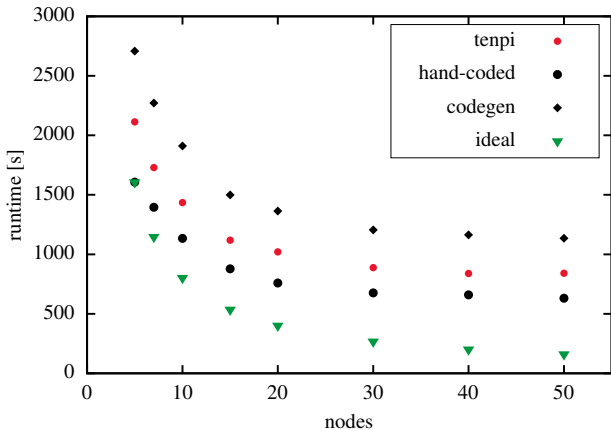


FIG. 8. Strong scaling benchmark on UF_6 . Average timing of a relativistic CCSD iteration with respect to the number of Summit nodes (6 GPUs per node). AS(66, 190).

To investigate the influence of the internode communication, we then moved to analyze the weak scaling of the code. Using the same system and method as previously, we varied the size of virtual space such that the number of operations per node is kept fixed, based on expected CCSD scaling

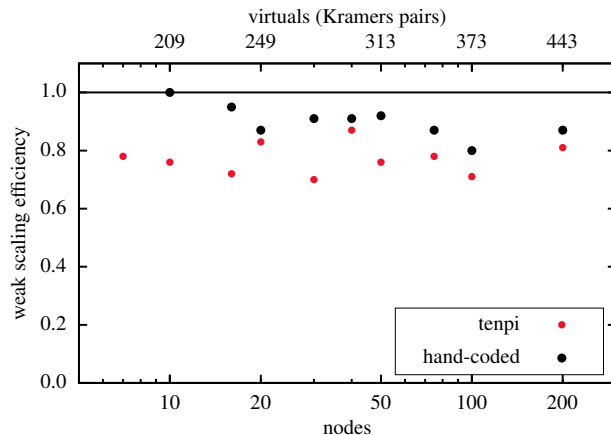


FIG. 9. Weak scaling behaviour of CCSD on UF_6 (relative to the smallest possible run) with respect to the number of Summit nodes (6 GPUs per node). In weak scaling, we increase the number of virtuals such that the workload per node remains constant, based on the naive computational scaling of CCSD. The number of occupied orbitals is fixed at 33.

of $\mathcal{O}(o^2v^4)$ with o the number of occupied and v of virtual spinors. The weak scaling efficiency is again calculated as t_1/t_N . The ideal weak scaling efficiency would be a constant 1.

As demonstrated in Fig. 9, the code exhibits a relatively constant weak scaling behavior to up to 200 nodes, meaning that it can be used efficiently on up to 1200 GPUs. This is a pleasing result for a code without hand-tuning. We attribute most fluctuations in the graph to differing appropriateness of fixed block size of 75^n elements used in case of CCSD when distributing the tensors, where n is the number of indices. Some virtual sizes come with smaller number of padding zeroes than others. Moreover, the handwritten code has different intermediates than tenpi and the advantage can differ for different space sizes. One could profile and hand-tune the generated code based on several test runs, but such non-systematic intervention would go against the design principles. Instead, using measured walltimes to improve the cost model in the optimization step is a subject of further study.

C. Application: CO

The CO molecule was chosen due to the interesting aspects of its triple bond stretching, studied in recent works of the Shabaev group¹³⁰ and Koput.¹³¹ In the former work, the influence of quantum electrodynamics (QED) corrections is analyzed which is relevant for the HAMP-vQED project³⁵ for which the present code was created. These are minute effects and their study requires highly accurate methods.

Fig. 10 shows the ground state energies up to the CCSDT level for the bond distance stretching from 0.8 to 1.85 Å. Fig. 11 shows similar results for up to CCSDTQ level with a smaller space.

As expected, single-reference methods struggle at large

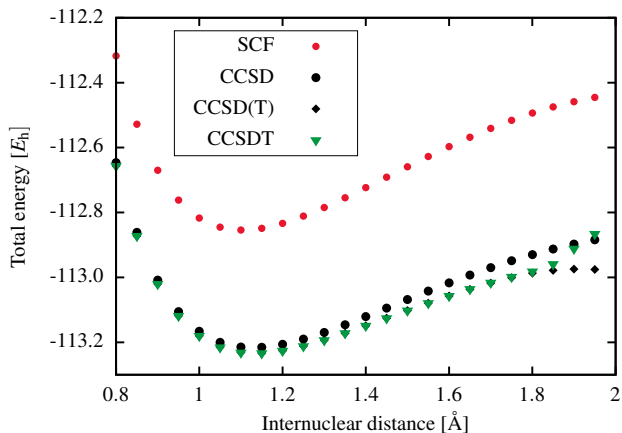


FIG. 10. Carbon monoxide ground state energy with full virtual space, AS(10,82), X2C Hamiltonian with amfX2C correction. Calculated on Summit using multi-node ExaTENSOR library.

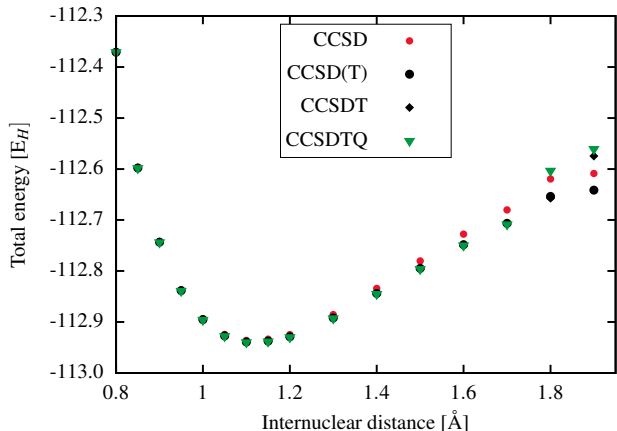


FIG. 11. Carbon monoxide ground state energy in small space AS(6,10), X2C Hamiltonian with amfX2C correction. Calculated on Frontier using single node multi-GPU TAL-SH library.

bond distances. The nonparallelity of CCSD and CCSDT becomes apparent at the bond distance of 1.75 Å (Fig. 10) and the CC has convergence issues from 1.85 Å on. This is also visible for the rightmost two points for CCSDTQ in Fig. 11.

A deeper study of the behavior of higher-order CC upon dissociation, and especially analyzing the minimum CC excitation level to break the bond successfully is beyond the scope of this manuscript, and will be a subject for our further work, once index-permutation symmetry of tensors is fully implemented.

V. CONCLUSIONS

tenpi is an open-source code generator published under BSD-3 license.³³ tenpi addresses the complex challenge of implementing coupled cluster for modern GPU based HPC platforms in a software-architecture sound way.

The code generated from tenpi is the first working implementation of CCSDT and CCSDTQ in DIRAC. Excellent weak scaling behavior is demonstrated with up to 1200 GPUs. For massively parallel CCSD, the performance is comparable to the hand-tuned code with the measured overhead of only 30%, which is an improvement over the 80% overhead of the existing generated CCSD. The code generation and optimization itself is fast relative to similar toolchains up to quadruple level.

Overall, the tenpi framework provides users with an elegant and systematic way of implementing the coupled cluster methods while hiding under the hood most of the complexity related to the equations, parallelization and intermediates. A simple python interface is featured, while the output is a highly optimized Fortran code that controls the parallel tensor library.

The stretching of the triple bond of CO was studied with convergence problems observed for higher-order CC, particularly for CCSDTQ at larger bond distances.

The outlook for tenpi includes the development of CCSD(T)¹³² and CCSDT(Q)¹³³ for distributed-GPU platforms, and addressing the current limitations like the lack of spatial-symmetry support and integration of DIRAC with tensor software that supports index-permutation symmetry. Inclusion of internode communication and real-world performance data into the cost model for intermediate optimization will be studied. The method development can be boosted by a symbolic interface to Mathematica. tenpi can also serve as a standalone production CC package, if the integral generation is interfaced directly to an existing code, like ReSpect.¹³⁴

Besides the above, this work maps the latest developments in relevant tensor software and shows how is the transition to a systematic development pipeline necessary to sustain modern coupled cluster codes.

ACKNOWLEDGMENTS

We very much acknowledge the consultations and support from André S.P. Gomes, Dmitry Lyakh, Jiří Pittner, Marcus Wagner, Lucas Visscher, Gabriele Fabbro and Paolo Bientinesi. This project has received funding from the the European Research Council (ERC) under the European Union’s Horizon 2020 research and innovation programme (grant agreement No 101019907). This research used resources of the Oak Ridge Leadership Computing Facility at the Oak Ridge National Laboratory, which is supported by the Office of Science of the U.S. Department of Energy under Contract No. DE-AC05-00OR22725. This work was granted access to the HPC resources of CALMIP supercomputing center under the allocation 2023-p13154 and 2024-M24070. We acknowledge VSB – Technical University of Ostrava, IT4Innovations National Supercomputing Center, Czech Republic, for awarding this project access to the LUMI supercomputer, owned by the EuroHPC Joint Undertaking, hosted by CSC (Finland) and the LUMI consortium through the Ministry of Education, Youth and Sports of the Czech Republic through the e-INFRA CZ (grant ID: 90254). We acknowledge the use of the MRCC

package^{124,125} and its CC methods.^{34,126}

- ¹TOP500.org, “TOP500 list,” <https://www.top500.org> (2024), [Online; accessed 06-Sep-2024].
- ²J. Dongarra, “A Not So Simple Matter of Software,” <https://www.hpcwire.com/2022/11/16/jack-dongarra-a-not-so-simple-matter-of-software/> (2023).
- ³F. Chirigati, *Nature Computational Science* **2**, 211–212 (2022).
- ⁴J. A. Calvin, C. Peng, V. Rishi, A. Kumar, and E. F. Valeev, *Chemical Reviews* **121**, 1203 (2021).
- ⁵W. Ma, S. Krishnamoorthy, and G. Agrawal, “Practical Loop Transformations for Tensor Contraction Expressions on Multi-level Memory Hierarchies,” in *Compiler Construction* (Springer Berlin Heidelberg, 2011) p. 266–285.
- ⁶C. Woolston, “Why science needs more research software engineers,” <http://dx.doi.org/10.1038/d41586-022-01516-2> (May 31 2022).
- ⁷D. I. Lyakh, *International Journal of Quantum Chemistry* **119**, 25926 (2019).
- ⁸S. Thibault, *On Runtime Systems for Task-based Programming on Heterogeneous Platforms*, *Habilitation à diriger des recherches*, Université de Bordeaux (2018).
- ⁹E. Rojas, E. Meneses, T. Jones, and D. Maxwell, in *2019 31st International Symposium on Computer Architecture and High Performance Computing (SBAC-PAD)* (IEEE, 2019).
- ¹⁰D. Zhao, S. Samsi, J. McDonald, B. Li, D. Bestor, M. Jones, D. Tiwari, and V. Gadepally, in *Proceedings of the 2023 ACM Symposium on Cloud Computing*, SoCC ’23 (ACM, 2023).
- ¹¹T. A. Heffernan and A. McKay, *Professional Development in Education* **45**, 102–113 (2018).
- ¹²“Summit User Guide,” https://docs.olcf.ornl.gov/systems/summit_user_guide.html (2024), [Online; accessed 27-May-2024].
- ¹³M. H. Lechner, A. Papadopoulos, K. Sivalingam, A. A. Auer, A. Koslowski, U. Becker, F. Wennmohs, and F. Neese, *Physical Chemistry Chemical Physics* **26**, 15205–15220 (2024).
- ¹⁴A. Papadopoulos, *Necessity of Code Generators in Electronic-Structure Theories and their Infrastructure*, *Master’s thesis*, University of Amsterdam, Amsterdam, Netherlands (2019).
- ¹⁵A. A. Auer, G. Baumgartner, D. E. Bernholdt, A. Bibireata, V. Choppella, D. Cociorva, X. Gao, R. Harrison, S. Krishnamoorthy, S. Krishnan, C.-C. Lam, Q. Lu, M. Nooijen, R. Pitzer, J. Ramanujam, P. Sadayappan, and A. Sibiryakov, *Molecular Physics* **104**, 211–228 (2006).
- ¹⁶The Mathworks, Inc., “MATLAB,” <https://mathworks.com/products/matlab.html> (2024).
- ¹⁷Waterloo Maple, Inc., “Maple,” <https://www.maplesoft.com/products/Maple/> (2024).
- ¹⁸Wolfram Research, Inc., “Mathematica, Version 14.0,” <https://www.wolfram.com/mathematica> (2024), Champaign, IL.
- ¹⁹The Khronos Group, Inc., “SYCL,” <https://www.khronos.org/sycl/> (2021).
- ²⁰The OpenACC Organization, “OpenACC,” <https://www.openacc.org> (2022).
- ²¹C. Augonnet, S. Thibault, R. Namyst, and P.-A. Wacrenier, *Concurrency and Computation: Practice and Experience Euro-Par 2009 best papers*, **23**, 187 (2011).
- ²²T. Herault, Y. Robert, G. Bosilca, R. J. Harrison, C. A. Lewis, E. F. Valeev, and J. J. Dongarra, in *2021 IEEE International Parallel and Distributed Processing Symposium (IPDPS)* (IEEE, 2021).
- ²³R. J. Harrison, G. Beylkin, F. A. Bischoff, J. A. Calvin, G. I. Fann, J. Fosso-Tande, D. Galindo, J. R. Hammond, R. Hartman-Baker, J. C. Hill, J. Jia, J. S. Kottmann, M.-J. Yvonne Ou, J. Pei, L. E. Ratcliff, M. G. Reuter, A. C. Richie-Halford, N. A. Romero, H. Sekino, W. A. Shelton, B. E. Sundahl, W. S. Thornton, E. F. Valeev, A. Vazquez-Mayagoitia, N. Vence, T. Yanai, and Y. Yokoi, *SIAM Journal on Scientific Computing* **38**, S123–S142 (2016).
- ²⁴M. Bauer, S. Treichler, E. Slaughter, and A. Aiken, in *2012 International Conference for High Performance Computing, Networking, Storage and Analysis* (IEEE, 2012).
- ²⁵R. Yadav, A. Aiken, and F. Kjolstad, in *Proceedings of the 43rd ACM SIGPLAN International Conference on Programming Language Design and Implementation* (ACM, 2022).
- ²⁶A. D. Bochevarov, E. F. Valeev, and C. David Sherrill, *Molecular Physics* **102**, 111–123 (2004).
- ²⁷T. Shiozaki, M. Kamiya, S. Hirata, and E. F. Valeev, *Physical Chemistry Chemical Physics* **10**, 3358 (2008).
- ²⁸V. Lotrich, N. Flocke, M. Ponton, B. A. Sanders, E. Deumens, R. J. Bartlett, and A. Perera, in *Proceedings of the 23rd international conference on Supercomputing*, ICS ’09 (ACM, 2009).
- ²⁹D. A. Matthews, *Molecular Physics* **117**, 1325–1333 (2018).
- ³⁰L. Zheng *et al.*, “Awesome Tensor Compilers,” <https://github.com/merrymercy/awesome-tensor-compilers> (2024).
- ³¹A. Panyala, *Search-based Model-driven Loop Optimizations for Tensor Contractions*, *Ph.D. thesis*, Louisiana State University Libraries (2014).
- ³²J. Brandejs, P. Bientinesi, L. Visscher, A. Gomes, and T. Saue, “CE-CAM Workshop on Tensor Contraction Library Standardization,” <https://tensor.sciencesconf.org/> (2024).
- ³³J. Brandejs and T. Saue, “tenpi: Tensor Programming Interface,” <https://gitlab.com/janbrandejs/tenpi> (2024).
- ³⁴M. Kállay and P. R. Surján, *The Journal of Chemical Physics* **115**, 2945–2954 (2001).
- ³⁵T. Saue *et al.*, “HAMP-vQED,” <https://dirac.ups-tlse.fr/hamp-vqed/doku.php?id=public:overview> (2024).
- ³⁶P.-W. Lai, H. Zhang, S. Rajbhandari, E. Valeev, K. Kowalski, and P. Sadayappan, *Procedia Computer Science* **9**, 412–421 (2012).
- ³⁷G. Baumgartner, A. Auer, D. Bernholdt, A. Bibireata, V. Choppella, D. Cociorva, X. Gao, R. Harrison, S. Hirata, S. Krishnamoorthy, S. Krishnan, C.-C. Lam, Q. Lu, M. Nooijen, R. Pitzer, J. Ramanujam, P. Sadayappan, and A. Sibiryakov, *Proceedings of the IEEE* **93**, 276–292 (2005).
- ³⁸R. A. Kendall, E. Aprà, D. E. Bernholdt, E. J. Bylaska, M. Dupuis, G. I. Fann, R. J. Harrison, J. Ju, J. A. Nichols, J. Niylocha, T. Straatsma, T. L. Windus, and A. T. Wong, *Computer Physics Communications* **128**, 260–283 (2000).
- ³⁹C. L. Janssen and H. F. Schaefer, *Theoretica Chimica Acta* **79**, 1–42 (1991).
- ⁴⁰X. Li and J. Paldus, *The Journal of Chemical Physics* **101**, 8812–8826 (1994).
- ⁴¹M. Nooijen and V. Lotrich, *Journal of Molecular Structure: THEOCHEM* **547**, 253–267 (2001).
- ⁴²E. Deumens, V. F. Lotrich, A. S. Perera, R. J. Bartlett, N. Jindal, and B. A. Sanders, “The Super Instruction Architecture,” in *Annual Reports in Computational Chemistry* (Elsevier, 2011) p. 179–191.
- ⁴³D. Ozog, J. R. Hammond, J. Dinan, P. Balaji, S. Shende, and A. Malony, in *2013 42nd International Conference on Parallel Processing* (IEEE, 2013) p. 30–39.
- ⁴⁴Y. Shao, L. F. Molnar, Y. Jung, J. Kussmann, C. Ochsenfeld, S. T. Brown, A. T. Gilbert, L. V. Slipchenko, S. V. Levchenko, D. P. O’Neill, R. A. DiStasio Jr, R. C. Lochan, T. Wang, G. J. Beran, N. A. Besley, J. M. Herbert, C. Yeh Lin, T. Van Voorhis, S. Hung Chien, A. Sodt, R. P. Steele, V. A. Rassolov, P. E. Maslen, P. P. Korambath, R. D. Adamson, B. Austin, J. Baker, E. F. C. Byrd, H. Dachsel, R. J. Doerksen, A. Dreuw, B. D. Dunietz, A. D. Dutoi, T. R. Furlani, S. R. Gwaltney, A. Heyden, S. Hirata, C.-P. Hsu, G. Kedziora, R. Z. Khallulin, P. Klunzinger, A. M. Lee, M. S. Lee, W. Liang, I. Lotan, N. Nair, B. Peters, E. I. Proynov, P. A. Pieniazek, Y. Min Rhee, J. Ritchie, E. Rosta, C. D. Sherrill, A. C. Simmonett, J. E. Subotnik, H. Lee Woodcock III, W. Zhang, A. T. Bell, A. K. Chakraborty, D. M. Chipman, F. J. Keil, A. Warshel, W. J. Hehre, H. F. Schaefer III, J. Kong, A. I. Krylov, P. M. W. Gill, and M. Head-Gordon, *Phys. Chem. Chem. Phys.* **8**, 3172–3191 (2006).
- ⁴⁵E. Epifanovsky, M. Wormit, T. Kuš, A. Landau, D. Zuev, K. Khistyayev, P. Manohar, I. Kaliman, A. Dreuw, and A. I. Krylov, *Journal of Computational Chemistry* **34**, 2293–2309 (2013).
- ⁴⁶E. Solomonik, D. Matthews, J. Hammond, and J. Demmel, in *2013 IEEE 27th International Symposium on Parallel and Distributed Processing* (IEEE, 2013).
- ⁴⁷J. A. Calvin, C. A. Lewis, and E. F. Valeev, in *Proceedings of the 5th Workshop on Irregular Applications: Architectures and Algorithms*, SC15 (ACM, 2015).
- ⁴⁸A. Irmeler, R. Kanakagiri, S. T. Ohlmann, E. Solomonik, and A. Grüneis, “Optimizing Distributed Tensor Contractions Using Node-Aware Pro-

- cessor Grids,” in *Euro-Par 2023: Parallel Processing* (Springer Nature Switzerland, 2023) p. 710–724.
- ⁴⁹I. Shavitt and R. J. Bartlett, *Many-Body Methods in Chemistry and Physics: MBPT and Coupled-Cluster Theory* (Cambridge University Press, 2009).
- ⁵⁰S. A. Kucharski and R. J. Bartlett, *The Journal of Chemical Physics* **97**, 4282–4288 (1992).
- ⁵¹T. Shiozaki, *WIREs Computational Molecular Science* **8**, 1331 (2017).
- ⁵²J. Goldstone, *Proceedings of the Royal Society of London. Series A. Mathematical and Physical Sciences* **239**, 267–279 (1957).
- ⁵³J. W. Park and T. Shiozaki, *Journal of Chemical Theory and Computation* **13**, 3676–3683 (2017).
- ⁵⁴F. Neese, *WIREs Computational Molecular Science* **12** (2022), 10.1002/wcms.1606.
- ⁵⁵M. Krupička, K. Sivalingam, L. Huntington, A. A. Auer, and F. Neese, *Journal of Computational Chemistry* **38**, 1853–1868 (2017).
- ⁵⁶R. Song, T. M. Henderson, and G. E. Scuseria, *The Journal of Chemical Physics* **156**, 104105 (2022).
- ⁵⁷M. Saitow, Y. Kurashige, and T. Yanai, *The Journal of Chemical Physics* **139**, 044118 (2013).
- ⁵⁸E. Neuscammen, T. Yanai, and G. K.-L. Chan, *The Journal of Chemical Physics* **130**, 124102 (2009).
- ⁵⁹O. Backhouse, “ebcc,” <https://github.com/BoothGroup/ebcc> (2024).
- ⁶⁰A. Köhn, G. W. Richings, and D. P. Tew, *The Journal of Chemical Physics* **129**, 201103 (2008).
- ⁶¹E. Solomonik, D. Matthews, J. R. Hammond, J. F. Stanton, and J. Demmel, *Journal of Parallel and Distributed Computing* **74**, 3176–3190 (2014).
- ⁶²D. G. A. Smith and J. Gray, *Journal of Open Source Software* **3**, 753 (2018).
- ⁶³R. Quintero-Monsebaiz and P.-F. Loos, *AIP Advances* **13**, 085035 (2023).
- ⁶⁴D. I. Lyakh, V. V. Ivanov, and L. Adamowicz, *The Journal of Chemical Physics* **122**, 024108 (2004).
- ⁶⁵Z. Wang, B. G. Peyton, and T. D. Crawford, *Journal of Chemical Theory and Computation* **18**, 5479–5491 (2022).
- ⁶⁶L. Chi-Chung, P. Sadayappan, and R. Wenger, *Parallel Processing Letters* **07**, 157–168 (1997).
- ⁶⁷L. Ma, J. Ye, and E. Solomonik, in *Proceedings of the ACM International Conference on Parallel Architectures and Compilation Techniques*, PACT ’20 (ACM, 2020).
- ⁶⁸A. Harju, T. Siro, F. F. Canova, S. Hakala, and T. Rantalaiho, “Computational Physics on Graphics Processing Units,” in *Lecture Notes in Computer Science* (Springer Berlin Heidelberg, 2013) p. 3–26.
- ⁶⁹X. Gao, S. Krishnamoorthy, S. K. Sahoo, C.-C. Lam, G. Baumgartner, J. Ramanujam, and P. Sadayappan, “Efficient Search-Space Pruning for Integrated Fusion and Tiling Transformations,” in *Lecture Notes in Computer Science* (Springer Berlin Heidelberg, 2006) p. 215–229.
- ⁷⁰S. Sahoo, S. Krishnamoorthy, R. Panuganti, and P. Sadayappan, in *ACM/IEEE SC 2005 Conference (SC’05)* (IEEE, 2005).
- ⁷¹R. Yadav, M. Bauer, D. Broman, M. Garland, A. Aiken, and F. Kjolstad, “Automatic Tracing in Task-Based Runtime Systems,” <https://arxiv.org/abs/2406.18111> (2024), arXiv:2406.18111 [cs.DC].
- ⁷²J. Johnson, R. W. Johnson, D. A. Padua, and J. Xiong, “Searching for the Best FFT Formulas with the SPL Compiler,” in *Lecture Notes in Computer Science* (Springer Berlin Heidelberg, 2001) p. 112–126.
- ⁷³E. Meiroim, H. Maron, S. Mannor, and G. Chechik, in *International Conference on Machine Learning* (PMLR, 2022) pp. 15278–15292.
- ⁷⁴U. Bondhugula, A. Hartono, J. Ramanujam, and P. Sadayappan, *ACM SIGPLAN Notices* **43**, 101–113 (2008).
- ⁷⁵P.-W. Lai, K. Stock, S. Rajbhandari, S. Krishnamoorthy, and P. Sadayappan, in *Proceedings of the International Conference on High Performance Computing, Networking, Storage and Analysis*, SC13 (ACM, 2013).
- ⁷⁶C. Psarras, L. Karlsson, J. Li, and P. Bientinesi, “The landscape of software for tensor computations,” <https://arxiv.org/abs/2103.13756> (2022), arXiv:2103.13756 [cs.MS].
- ⁷⁷D. A. Matthews, *SIAM Journal on Scientific Computing* **40**, C1 (2018).
- ⁷⁸J. Brabec, J. Brandejs, K. Kowalski, S. Xantheas, O. Legeza, and L. Veis, *Journal of Computational Chemistry* **42**, 534–544 (2020).
- ⁷⁹C. Peng, J. A. Calvin, F. Pavošević, J. Zhang, and E. F. Valeev, *The Journal of Physical Chemistry A* **120**, 10231 (2016).
- ⁸⁰R. Levy, E. Solomonik, and B. K. Clark, in *SC20: International Conference for High Performance Computing, Networking, Storage and Analysis* (IEEE, 2020).
- ⁸¹D. I. Lyakh, T. Nguyen, D. Claudino, E. Dumitrescu, and A. J. McCaskey, *Frontiers in Applied Mathematics and Statistics* **8**, 838601 (2022).
- ⁸²O. Sharir, A. Shashua, and G. Carleo, *Physical Review B* **106**, 205136 (2022).
- ⁸³E. C. Chi and T. G. Kolda, *SIAM Journal on Matrix Analysis and Applications* **33**, 1272 (2012).
- ⁸⁴N. D. Sidiropoulos, L. D. Lathauwer, X. Fu, K. Huang, E. E. Papalexakis, and C. Faloutsos, *IEEE Transactions on Signal Processing* **65**, 3551 (2017).
- ⁸⁵Y. Shi, U. N. Niranjan, A. Anandkumar, and C. Cecka, in *2016 IEEE 23rd International Conference on High Performance Computing (HiPC)* (IEEE, 2016).
- ⁸⁶E. Georganas, D. Kalamkar, S. Avancha, M. Adelman, C. Anderson, A. Breuer, J. Bruestle, N. Chaudhary, A. Kundu, D. Kutnick, F. Laub, V. Md, S. Misra, R. Mohanty, H. Pabst, B. Ziv, and A. Heinecke, in *Proceedings of the International Conference for High Performance Computing, Networking, Storage and Analysis* (ACM, 2021).
- ⁸⁷P. Springer and P. Bientinesi, “Design of a high-performance GEMM-like Tensor-Tensor Multiplication,” <https://arxiv.org/abs/1607.00145> (2017), arXiv:1607.00145 [cs.MS].
- ⁸⁸“NVIDIA cuTENSOR: A High-Performance CUDA Library For Tensor Primitives,” <https://docs.nvidia.com/cuda/cutensor/latest/index.html> (2019).
- ⁸⁹P. Bientinesi, D. Ham, F. Huang, P. H. J. Kelly, P. S. Sadayappan, and E. Stow, *Dagstuhl Reports*, 1 (2022).
- ⁹⁰E. Valeev, “Basic Programming of TiledArray,” https://valeevgroup.github.io/tiledarray/dox-master/_basic_programming.html (2023), [Online; accessed 13-July-2023].
- ⁹¹cppreference.com community, “C++ reference MDSPAN,” <https://en.cppreference.com/w/cpp/container/mdspan> (2023), [Online; accessed 13-July-2023].
- ⁹²R. Murray, J. Demmel, M. W. Mahoney, N. B. Erichson, M. Melnichenko, O. A. Malik, L. Grigori, P. Luszczek, M. Dereziński, M. E. Lopes, T. Liang, H. Luo, and J. Dongarra, “Randomized Numerical Linear Algebra : A Perspective on the Field With an Eye to Software,” <https://arxiv.org/abs/2302.11474> (2023), arXiv:2302.11474 [math.NA].
- ⁹³TAPP working group, “Tensor Algebra Processing Primitives,” <https://github.com/TAPPorg/tensor-interfaces> (2024).
- ⁹⁴J. V. Pototschnig, A. Papadopoulos, D. I. Lyakh, M. Repisky, L. Halbert, A. S. P. Gomes, H. J. Aa. Jensen, and L. Visscher, *Journal of Chemical Theory and Computation* **17**, 5509 (2021).
- ⁹⁵“TAL-SH,” https://github.com/DmitryLyakh/TAL_SH (2018).
- ⁹⁶E. Mutlu, A. Panyala, N. Gawande, A. Bagussety, J. Glabe, J. Kim, K. Kowalski, N. P. Bauman, B. Peng, H. Pathak, J. Brabec, and S. Krishnamoorthy, *The Journal of Chemical Physics* **159**, 024801 (2023).
- ⁹⁷B. Palmer, E. Apra, A. Panyala, J. Hammond, C. Pe, and S. Krishnamoorthy, “GlobalArrays,” <https://github.com/GlobalArrays/ga> (2022).
- ⁹⁸T. Zhang, X.-Y. Liu, X. Wang, and A. Walid, *IEEE Transactions on Parallel and Distributed Systems* **31**, 595 (2020).
- ⁹⁹C. Millette, C. Ma, and M. Karunanidhi, “hipTensor,” <https://github.com/ROCM/hipTensor> (2024).
- ¹⁰⁰A. Paszke, S. Gross, F. Massa, A. Lerer, J. Bradbury, G. Chanan, T. Killeen, Z. Lin, N. Gimelshein, L. Antiga, A. Desmaison, A. Kopf, E. Yang, Z. DeVito, M. Raison, A. Tejani, S. Chilamkurthy, B. Steiner, L. Fang, J. Bai, and S. Chintala, in *Advances in Neural Information Processing Systems 32* (Curran Associates, Inc., 2019) pp. 8024–8035.
- ¹⁰¹M. Abadi, in *Proceedings of the 21st ACM SIGPLAN International Conference on Functional Programming* (ACM, 2016).
- ¹⁰²T. D. Crawford and H. F. Schaefer, *Reviews in Computational Chemistry* **14**, 33 (2000).
- ¹⁰³D. Kats, “CCDiag - Coupled-Cluster diagrams in LaTeX,” <https://github.com/fkfest/ccdiag> (2024).
- ¹⁰⁴A. Meurer, C. P. Smith, M. Paprocki, O. Čertík, S. B. Kirpichev, M. Rocklin, A. Kumar, S. Ivanov, J. K. Moore, S. Singh, T. Rathnayake, S. Vig, B. E. Granger, R. P. Muller, F. Bonazzi, H. Gupta, S. Vats, F. Johansson, F. Pedregosa, M. J. Curry, A. R. Terrel, v. Roučka, A. Saboo, I. Fernando, S. Kulal, R. Cimrman, and A. Scopatz, *PeerJ Computer Science* **3**, e103

- (2017).
- ¹⁰³L. Visscher, H. J. Aa. Jensen, R. Bast, A. S. P. Gomes, T. Saue, I. A. Aucar, V. Bakken, J. Brandeys, C. Chibueze, J. Creutzberg, K. G. Dyall, S. Dubillard, U. Ekström, E. Eliav, T. Enevoldsen, E. Faßhauer, T. Fleig, O. Fossgaard, L. Halbert, E. D. Hedegård, T. Helgaker, B. Helmich-Paris, J. Henriksson, M. van Horn, M. Iliaš, C. R. Jacob, S. Knecht, S. Komorovský, O. Kullie, J. K. Lærdahl, C. V. Larsen, Y. S. Lee, N. H. List, H. S. Nataraj, M. K. Nayak, P. Norman, A. Nyvang, M. Olejniczak, J. Olsen, J. M. H. Olsen., A. Papadopoulos, Y. C. Park, J. K. Pedersen, M. Pernpointner, J. V. Pototschnig, R. Di Remigio Eikås, M. Repisky, K. Ruud, P. Salek, B. Schimmelpfennig, B. Senjean, A. Shee, J. Sikkema, A. Sunaga, J. Thyssen, J. van Stralen, M. L. Vidal, S. Villaume, O. Visser, T. Winther, S. Yamamoto, and X. Yuan, “DIRAC24,” <https://zenodo.org/doi/10.5281/zenodo.10680560> (2024).
- ¹⁰⁶T. Saue, R. Bast, A. S. P. Gomes, H. J. Aa. Jensen, L. Visscher, I. A. Aucar, R. Di Remigio, K. G. Dyall, E. Eliav, E. Fasshauer, T. Fleig, L. Halbert, E. D. Hedegård, B. Helmich-Paris, M. Iliaš, C. R. Jacob, S. Knecht, J. K. Laerdahl, M. L. Vidal, M. K. Nayak, M. Olejniczak, J. M. H. Olsen, M. Pernpointner, B. Senjean, A. Shee, A. Sunaga, and J. N. P. van Stralen, *The Journal of Chemical Physics* **152**, 204104 (2020).
- ¹⁰⁷NEC, “NEC receives order for next-generation supercomputer system from Japan’s National Institutes for Quantum Science and Technology and National Institute for Fusion Science,” https://www.nec.com/en/press/202411/global_20241113_02.html (2024).
- ¹⁰⁸Hewlett Packard Enterprise (HPE), “Cray MPICH,” <https://www.mpich.org/static/docs/slides/2023-sc-bof/HPE.pdf> (2023).
- ¹⁰⁹J. Sucher, *Phys. Rev. A* **22**, 348 (1980).
- ¹¹⁰A. Almoukhalalati, S. Knecht, H. J. A. Jensen, K. G. Dyall, and T. Saue, *The Journal of Chemical Physics* **145**, 074104 (2016).
- ¹¹¹H. J. Aa. Jensen, (2005), *Douglas-Kroll the Easy Way*, Talk at Conference on Relativistic Effects in Heavy Elements - REHE, Mülheim, Germany, April, 2005. Available at <https://doi.org/10.6084/m9.figshare.12046158>.
- ¹¹²W. Kutzelnigg and W. Liu, *J. Chem. Phys.* **123**, 241102 (2005).
- ¹¹³M. Iliaš and T. Saue, *J. Chem. Phys.* **126**, 064102 (2007).
- ¹¹⁴W. Liu and D. Peng, *J. Chem. Phys.* **131**, 031104 (2009).
- ¹¹⁵B. A. Hess, C. M. Marian, U. Wahlgren, and O. Gropen, *Chem. Phys. Lett.* **251**, 365 (1996).
- ¹¹⁶B. Schimmelpfennig, “*AMFI, an atomic mean-field spin-orbit integral program*,” University of Stockholm, Stockholm, Sweden; 1996.
- ¹¹⁷S. Knecht, M. Repisky, H. J. Aa. Jensen, and T. Saue, *The Journal of Chemical Physics* **157**, 114106 (2022).
- ¹¹⁸K. G. Dyall, “Dyall dz, tz, and qz basis sets for relativistic electronic structure calculations,” <https://doi.org/10.5281/zenodo.7574629> (2023).
- ¹¹⁹T. H. Dunning, *J. Chem. Phys.* **90**, 1007 (1989).
- ¹²⁰X. Yuan, L. Visscher, and A. S. P. Gomes, *The Journal of Chemical Physics* **156**, 224108 (2022).
- ¹²¹J. S. Binkley, J. A. Pople, and W. J. Hehre, *J. Am. Chem. Soc.* **102**, 939 (1980).
- ¹²²J. D. Dill and J. A. Pople, *J. Chem. Phys.* **62**, 2921 (1975).
- ¹²³R. Ditchfield, W. J. Hehre, and J. A. Pople, *J. Chem. Phys.* **54**, 724 (1971).
- ¹²⁴M. Kállay, P. R. Nagy, D. Mester, Z. Rolik, G. Samu, J. Csontos, J. Csóka, P. B. Szabó, L. Gyevi-Nagy, B. Hégyely, I. Ladjánszki, L. Szegedy, B. Ladóczki, K. Petrov, M. Farkas, P. D. Mezei, and Á. Ganyecz, *J. Chem. Phys.* **152**, 074107 (2020).
- ¹²⁵“MRCC,” <https://www.mrcc.hu/> (2024), MRCC, a quantum chemical program suite written by M. Kállay, P. R. Nagy, D. Mester, L. Gyevi-Nagy, J. Csóka, P. B. Szabó, Z. Rolik, G. Samu, J. Csontos, B. Hégyely, Á. Ganyecz, I. Ladjánszki, L. Szegedy, B. Ladóczki, K. Petrov, M. Farkas, P. D. Mezei, and R. A. Horváth. See www.mrcc.hu.
- ¹²⁶M. Kállay, J. Gauss, and P. G. Szalay, *The Journal of Chemical Physics* **119**, 2991–3004 (2003).
- ¹²⁷L. Visscher, T. J. Lee, and K. G. Dyall, *The Journal of Chemical Physics* **105**, 8769–8776 (1996).
- ¹²⁸A. Gomes and D. I. Lyakh, “Relmbdev/mb-autogen: mb-autogen,” <https://zenodo.org/record/8094430> (2023).
- ¹²⁹G. M. Amdahl, *Computer* **46**, 38–46 (2013).
- ¹³⁰D. P. Usov, Y. S. Kozhedub, V. V. Meshkov, A. V. Stolyarov, N. K. Dulaev, A. M. Ryzhkov, I. M. Savelyev, V. M. Shabaev, and I. I. Tupitsyn, *Physical Review A* **109**, 042822 (2024).
- ¹³¹J. Koput, *Journal of Chemical Theory and Computation* **20**, 9041–9047 (2024).
- ¹³²K. Raghavachari, G. W. Trucks, J. A. Pople, and M. Head-Gordon, *Chemical Physics Letters* **589**, 37–40 (2013).
- ¹³³K. Kowalski and P. Piecuch, *The Journal of Chemical Physics* **113**, 18–35 (2000).
- ¹³⁴M. Repisky, S. Komorovsky, M. Kadek, L. Konecny, U. Ekström, E. Malkin, M. Kaupp, K. Ruud, O. L. Malkina, and V. G. Malkin, *The Journal of Chemical Physics* **152**, 184101 (2020).